Rhodopsin Photoproducts and Rod Sensitivity in the Skate Retina

KENNETH P. BRIN and HARRIS RIPPS

From the Departments of Ophthalmology and Physiology, New York University School of Medicine, New York 10016, and the Marine Biological Laboratory, Woods Hole, Massachusetts 02543

ABSTRACT The late photoproducts that result from the isomerization of rhodopsin have been identified in the isolated all-rod retina of the skate by means of rapid spectrophotometry. The sequence in which these intermediates form and decay could be described by a scheme that incorporates two pathways for the degradation of metarhodopsin II (MII) to retinol: one via metarhodopsin III (MIII) and the other (which bypasses MIII) through retinal. Computer simulation of the model yielded rate constants and spectral absorbance coefficients for the late photoproducts which fit experimental data obtained at temperatures ranging from 7°C to 27°C. Comparing the kinetics of the thermal reactions with the changes in rod threshold that occur during dark adaptation indicated that the decay of MII and the fall in receptor thresholds exhibit similarities with regard to their temperature dependence. However, the addition of 2 mM hydroxylamine to a perfusate bathing the retina greatly accelerated the photochemical reactions, but had no significant effect on the rate of recovery of rod sensitivity. It appears, therefore, that the late bleaching intermediates do not control the sensitivities of skate rods during dark adaptation.

INTRODUCTION

Spectrophotometry of the isolated vertebrate retina has shown that after a photically induced isomeric change in its chromophore, the rhodopsin molecule degrades thermally through several short-lived intermediates to metarhodopsin II (MII). The latter decays, in turn, at a much slower rate to other photoproducts before the chromophore is hydrolyzed from the protein moiety (opsin) and reduced to the relatively colorless retinol (vitamin A); at this stage, rhodopsin is said to have "bleached."

The reactions that follow the formation of MII take place too long after photic exposure to be involved in the initial transduction process. However, Donner and Reuter (1967, 1968) have suggested that one or more of the late photoproducts is responsible for regulating the sensitivity of the rod mechanism during the initial phase of the dark-adaptation process; i.e. the relatively rapid changes in threshold that occur independently of rhodopsin regeneration (Dowling, 1963). The nearly linear relation between the fall in log threshold and the exponential decay of intermediates with $\lambda_{max} \approx 380$ nm (i.e. MII and retinal) led them to the conclusion that these substances have a profound desensitizing effect on the

rods; e.g., 380-nm products equivalent to 1% of the total rhodopsin content of the rods raise threshold 2.0–2.5 log units (Donner, 1973). Further support for this notion stems from experimental studies (Donner and Reuter, 1967; Donner, 1973) showing that temperature variation induces similar changes in the rate constants of photoproduct decay and of dark adaptation.

Although Donner and Reuter's hypothesis has some attractive features, it should be noted that the threshold data referred to above were culled from recordings of the spike discharge of ganglion cells, elements located proximal to the site at which the photopigment changes occur. According to Frank (1971), the agreement between the kinetics of dark adaptation and photoproduct decay obtained at different temperatures may be fortuitous, e.g., sensitivity changes measured at the ganglion cell could perhaps reflect the effects of temperature on synaptic delay rather than on rod sensitivity. Moreover, the results obtained with other measures of retinal sensitivity suggest that long-lived photoproducts do not affect scotopic thresholds. For example, in the rat retina maintained at 30°C, Frank and Dowling (1968) have shown that the decay of the late bleaching intermediates (principally MII and MIII) takes about 40 min, whereas electroretinographic (*b*-wave) thresholds fall within the first 5 min after photic exposure to a level that is maintained for the duration of dark adaptation. And in the isolated, perfused retina of the frog, Frank (1971) reported that, unlike photoproduct kinetics, the electroretinal measures of receptor adaptation were insensitive to changes in temperature from 8° to 22°C.

It is apparent, therefore, that a question remains as to whether any of the substances formed during the decay of rhodopsin exerts a significant effect on retinal sensitivity or on the rate at which photoreceptors dark adapt. The issue is further complicated by the fact that there is little agreement as to the nature of the intermediates, their interconversions, and the rates at which they form and decay *in situ*, (Baumann, 1972; Frank, 1969; Matthews et al., 1963; Cone and Cobbs, 1969; Donner and Hemilä, 1975).

Our own approach to this problem has been to establish first the identity and kinetics of the late photoproducts, and then to determine whether any correlation that may exist between receptoral adaptation and photoproduct decay is retained when the rates of these reactions are manipulated either thermally or chemically. In all of this work we have chosen the skate as our experimental animal. The retina of this elasmobranch contains only rods (Dowling and Ripps, 1970; 1971*a*, 1972), a feature that eliminates any ambiguities introduced by the intrusion of cone-mediated responses. The first section of this paper presents the spectrophotometric data and analytical methods utilized in determining the rhodopsin decay pathways; the second deals with the comparison of photoproduct kinetics and receptoral thresholds during dark adaptation.

METHODS

The eyes of dark-adapted skates (*Raja erinacea* or *R. oscellata*) were enucleated under dim red illumination, the globe was hemisected, and the posterior segment was trimmed until only the highly reflective tapetal region remained. After the vitreous humor had been gently removed, the eyecup was cut into small squares (about 4 mm to the side) and placed in a beaker of oxygenated Ringer solution (see below). Immediately before an

experimental run the retina was detached from the eyecup and transferred to a perfusion chamber that electrically isolated its surfaces for the recording of transretinal potentials (Sickel, 1965). The perfusate, contained in an elevated bottle, was delivered to the chamber by gravity feed through intravenous drip tubing. Before reaching the inflow channel, a short length of the tubing was wrapped around the cooling element of a temperature control unit (FTS Systems, Stone Ridge, N.Y.) that maintained the perfusate at a constant preset value (5–27°C). The temperature in the chamber was measured before and after each experiment with a thermal probe (Yellow Springs Instrument Co., Yellow Springs, Ohio); the two measurements never differed by more than 0.5°C.

The perfusate for most experiments was a modified Ringer solution in which sodium aspartate was substituted for an equivalent amount of sodium chloride in order to isolate the PIII (receptoral) component of the electroretinogram (Sillman et al., 1969; Dowling and Ripps, 1972). The solution, oxygenated for at least 10 min before the start of an experiment and titrated with sodium hydroxide to pH 7.5, contained: NaCl, 230 mM; L-Na aspartate, 50 mM; KCl, 12 mM; $CaCl_2$, 10 mM; urea, 360 mM; glucose, 5.5 mM; $NaHCO_3$, 4.5 mM. Control runs in normal Ringer solution showed unequivocally that the aspartate had no effect on rhodopsin kinetics. In several experiments, hydroxylamine hydrochloride (2 mM) was added to the aspartate-Ringer solution.

Spectrophotometry

The perfusion chamber was mounted on the stage of a compound microscope for measurements of retinal transmissivity. Collimated light from a 150-W xenon arc lamp passed through a rotating wheel (5 rps) carrying 29 narrow-band interference filters spanning the spectrum from 360 nm to 720 nm. The beam was delimited by an aperture which was imaged in the plane of the retina by the microscope condenser. After traversing the retina, the measuring beam was collected by the microscope objective and channeled to the cathode of a photomultiplier (EMI 9558Q, Varian/EMI, Plainview, N. Y.). A hinged reflex viewer, interposed between the specimen and the phototube, was fitted with an IR image converter, enabling the observer to focus and align the preparation without affecting the pigment content or photosensitivity of the retina.

The signals from the photomultiplier fed a cathode follower, the output of which entered the analog-to-digital converter of a PDP-8/I computer (Digital Equipment Corp., Maynard, Mass.); the signals were displayed simultaneously on an oscilloscope as a series of 29 positive deflections, each corresponding to the wavelength of light derived from one of the spectral filters in the spinning wheel. The area under each of the deflections was approximated by converting the analog signals to digital values at brief, regular time intervals, and integrating these numbers by using the trapezoidal rule (for details see Ripps and Snapper, 1974); the data were stored in a temporary buffer, each in its appropriate wavelength bin. This process was repeated for eight complete spectral scans, after which averages and variances of the eight areas corresponding to each test wavelength were calculated and stored as one *time-vector*. Thus, a time vector contains the 29 transmissivity measurements (stored in 29 bins) obtained during the 1.5 s required to collect the eight spectral scans. Absorbance (density) differences were calculated from the time vectors according to the equation:

$$[\Delta dD_{1\text{-}2}]_\lambda = [\log_{10}(T_1/T_2)]_\lambda,$$

where T_1 and T_2 are the transmissivities (areas) at each wavelength λ within the time vectors 1 and 2. The absorbance difference spectrum represents, therefore, the wavelength variation in retinal transmissivity between scans recorded at times t_1 and t_2 (e.g., between a dark-adapted retina and one that has been exposed to light). Difference

spectra were plotted on a computer-driven storage scope (Tektronix 611, Roslyn Heights, N. Y.), and permanent records were provided by a hard copy unit (Tektronix 4601).

The Bleaching or ERG-Test Beam

A movable mirror that occluded the spectral measuring beam introduced light from a second heat-filtered xenon arc lamp that served as either a bleaching source or an ERG test stimulus. An electronic shutter gave accurately timed exposures: 100 ms for ERG test flashes, and 1 s for the rhodopsin bleaches. A Wratten 15 (yellow) filter (Eastman Kodak Corp., Rochester, N. Y.) with less than 1% transmission at wavelengths below 510 nm was inserted in this beam unless indicated otherwise. The incident energy of the bleaching source was measured in the plane of the retina with a calibrated radiometer (Yellow Springs Instrument Co., Yellow Springs, Ohio). Unattenuated, except for the Wratten 15 filter, the energy flux delivered by this source was 10.0 mW/cm^2. Neutral density filters, employed to further attenuate the beam, were calibrated with a Gilford spectrophotometer (Gilford Instrument Laboratories, Inc., Oberlin, Ohio).

Electrophysiology

Chlorided silver wires were embedded in either side of the central insert of the perfusion chamber to contact the solutions bathing the two sides of the retina. The electrodes were connected to a junction box which led to the differential inputs of a low noise preamplifier (Princeton Applied Research, Princeton, N. J.) set for a bandpass of 0.03–300 Hz. The transretinal responses were recorded on a Brush penwriter (Gould, Inc., Cleveland, Ohio); calibration signals were inserted before and after each experiment.

Experimental Procedure

A typical experimental protocol involved an equilibration period of 30–60 min during which electrical responses and transmissivity measurements were repeated to ensure stability of the preparation. A complete set of prebleach measurements were then obtained: two dark-adapted spectral time-vectors for photochemistry, and a complete intensity-response series for the electrophysiological experiments. It is important to note that in the dark-adapted retina, the 1.5–2.0-s exposure to the measuring beams of the spectrophotometer did not alter the absolute threshold of the receptor potential; and conversely, the retinal irradiance of the ERG test flashes was several log units below that required to bleach significant amounts of rhodopsin (cf. Dowling and Ripps, 1971*a*). After the data had been collected from the dark-adapted preparation, the retina was exposed to the bleaching light, and spectral and/or electrical measurements were recorded at various postexposure intervals.

ANALYSIS OF SPECTROPHOTOMETRIC DATA

Several of the decay pathways purported to describe the sequence of late thermal intermediates *in situ* were tested in the context of the present study. Each scheme was expressed in terms of a set of linearly independent equations representing the changes in concentration of the photoproducts in terms of the rate constants of the transitions between stages. The equations were solved explicitly, and with appropriate substitutions (see below) gave expressions for the spectral absorbance of each photoproduct as a function of time.

A set of computer programs utilizing an iterative, least-squares technique (cf. Draper and Smith, 1966) determined the rate constants and absorbance coefficients of the various intermediates which best satisfied the experimental data. Input to the programs consisted of the measured absorbance changes at a given wavelength and the times at which the individual measurements were made. The criterion for convergence of the iterative

process was satisfied when the correction factor for each parameter was less than 1×10^{-4} times the magnitude of the parameter itself. The mathematical analysis was simplified by assuming that: (*a*) each of the kinetic processes is a first-order reaction; (*b*) in the few seconds between photic exposure and measurement, all of the isomerized rhodopsin has been converted to MII, i.e., the concentration of other photoproducts is negligible; and (*c*) the sum of the relative concentrations of the particular photoproducts is always equal to the concentration of the rhodopsin bleached $[R_{bl}]$, i.e. no other intermediates are involved in the decay sequence. The rationale for these assumptions has been provided by Baumann (1972).

Pathways for the Decay of Late Photoproducts

One of the models tested which includes all of the late intermediates detectable in the isolated retina is a direct pathway (Ostroy et al., 1966) by which all the MII formed degrades via MIII to retinal (RAL), which is then reduced to retinol (ROL):

$$\mathrm{MII} \longrightarrow \mathrm{MIII} \longrightarrow \mathrm{RAL} \longrightarrow \mathrm{ROL}$$

$$\lambda_{max} = (380\ \mathrm{nm}) \quad (465\ \mathrm{nm}) \quad (387\ \mathrm{nm}) \quad (325\ \mathrm{nm}).$$

However, the evidence from a number of studies (Cone and Cobbs, 1969; Baumann, 1972; Donner and Hemilä, 1975) including our own (see below) indicates that MII decays *in situ* via two pathways, one of which includes MIII and the other of which bypasses this intermediate. By applying similar mathematical modeling and computer simulation techniques to absorbance measurements of the frog retina, Baumann (1972) found that his data were best fit by a model that incorporated a "shunt" pathway through which a fraction of the MII is hydrolyzed directly to retinal and opsin:

$$\mathrm{MII} \rightarrow \mathrm{MIII} \rightarrow \mathrm{RAL} \rightarrow \mathrm{ROL}.$$
$$\mathrm{MII} \rightarrow \mathrm{RAL}$$

Although Baumann's scheme adequately accounts for the fact that in the skate retina, as in the frog's, only a fraction of the MII that decays is transformed to MIII (cf. Fig. 1), the shunt model was unable to provide rate constants that fit the experimental data for the skate.

An alternative scheme, first proposed by Cone and Cobbs (1969) proved more satisfactory. Here, too, MII decays via two pathways, one to MIII, the other to retinal. But unlike the shunt model, retinol is formed from both retinal and MIII; i.e., MIII is not converted to retinal:

$$\mathrm{MII} \xrightarrow{k_1} \mathrm{MIII} \xrightarrow{k_2} \mathrm{ROL}$$
$$\mathrm{MII} \xrightarrow{k_4} \mathrm{RAL} \xrightarrow{k_3} \mathrm{ROL}$$

For this *dual pathway* model, the rates of change of the intermediates are given by the following differential equations:

$$\frac{d[\mathrm{MII}]}{dt} = [R_{bl}] \times \{-(k_1 + k_4)[\mathrm{MII}]\}, \tag{1}$$

$$\frac{d[\mathrm{MIII}]}{dt} = [R_{bl}] \times \{k_1[\mathrm{MII}] - k_2[\mathrm{MIII}]\}, \tag{2}$$

$$\frac{d[\mathrm{RAL}]}{dt} = [R_{bl}] \times \{k_4[\mathrm{MII}] - k_3[\mathrm{RAL}]\}, \tag{3}$$

$$\frac{d[\mathrm{ROL}]}{dt} = [R_{bl}] \times \{k_2[\mathrm{MIII}] + k_3[\mathrm{RAL}]\}, \tag{4}$$

where bracketed terms refer to the concentrations of the various substances. Solving the above gives the concentration values as a function of time t:

$$[\mathrm{MII}] = [R_{bl}] \times \{e^{-(k_1 + k_4)t}\}, \tag{5}$$

$$[\mathrm{MIII}] = [R_{bl}] \times \frac{k_1}{k_2 - (k_1 + k_4)} \{e^{-(k_1 + k_4)t} - e^{-k_2 t}\}, \tag{6}$$

$$[\mathrm{RAL}] = [R_{bl}] \times \frac{k_4}{k_3 - (k_1 + k_4)} \{e^{-(k_1 + k_4)t} - e^{-k_3 t}\}, \tag{7}$$

$$[\mathrm{ROL}] = [R_{bl}] \times \{1 - [\mathrm{MII}] - [\mathrm{MIII}] - [\mathrm{RAL}]\}. \tag{8}$$

It will be recalled, however, that the experimental measurements are expressed in absorbance units, not concentration. To convert to absorbance $(D_i)_\lambda$, the foregoing expressions are multiplied by $(\epsilon_i)_\lambda \times L$, where $(\epsilon_i)_\lambda$ is the molar extinction of intermediate i at wavelength λ, and L is the optical path length through the photoreceptors. Eq. (6) for example, can be written in the form:

$$(D_{\mathrm{MIII}})_{\lambda,t} = (\delta_{\mathrm{MIII}})_\lambda \left\{ \frac{k_1}{k_2 - (k_1 + k_4)} \left(e^{-(k_1 + k_4)t} - e^{-k_2 t} \right) \right\}, \tag{9}$$

where $(\delta_{\mathrm{MIII}})_\lambda$ is the absorbance coefficient and equal to $(\epsilon_i)_\lambda \times L \times [R_{bl}]$.

But our concern is with the change in absorbance (ΔD) at the test wavelength λ. This is obtained by summing the values of $(D_i)_\lambda$ for all photopigments contributing to the absorption at that λ, including the loss in absorbance resulting from the photolysis of rhodopsin $(\Delta D_{Rh})_\lambda$.

Thus, for λ = 470 nm, where the temporal changes in absorbance are due almost exclusively to MIII (Matthews et al., 1963; Baumann, 1972), the change in absorbance is given by the expression:

$$\begin{aligned}(\Delta D)_{470,t} &= (D_{\mathrm{MIII}})_{470,t} + (\Delta D_{Rh})_{470} \\ &= (\Delta_{\mathrm{MIII}})_{470} \left\{ \frac{k_1}{k_2 - (k_1 + k_4)} \left(e^{-(k_1 + k_4)t} - e^{-k_2 t} \right) \right\} + (\Delta D_{Rh})_{470}.\end{aligned} \tag{10}$$

And absorbance differences $(\Delta D)_t$ measured at 380 nm are described by considering MII, retinal, and rhodopsin (neither MIII nor retinol contributes significantly to the ΔD values at 380 nm), i.e.,

$$\begin{aligned}(\Delta D)_{380,t} = {} & (\delta_{\mathrm{MII}})_{380} \{e^{-(k_1 + k_4)t}\} \\ & + (\delta_{\mathrm{RAL}})_{380} \left\{ \frac{k_4}{k_3 - (k_1 + k_4)} \left(e^{-(k_1 + k_4)t} - e^{-k_3 t} \right) \right\} \\ & + (\Delta D_{Rh})_{380}.\end{aligned} \tag{11}$$

It should be noted that the parameters δ_{MIII} and k_1 of Eq. (10), as well as δ_{RAL} and k_4 of Eq. (11), are not independent. Consequently, regression analysis required a transformation of variables, described in the Appendix.

RESULTS

Absorbance Changes after Bleaching

Fig. 1 shows a typical set of difference spectra based on transmissivity measurements taken before and at the times indicated after a 1-s photic exposure to a retinal irradiance of 1.95 mW/cm^2. The difference spectrum obtained immedi-

ately after the flash (curve 1) reveals a loss in absorbance at wavelengths greater than 427 nm, and a commensurate gain in absorbance below this wavelength. The reduced absorbance (λ_{max} = 502 nm) is due clearly to a loss of rhodopsin, but the absorbance increase maximal at 380 nm may represent the formation of MII or retinal, or a combination of the two. Although not apparent in these data, rhodopsin may be presumed to have decayed through several intermediate states during the nearly 2 s between the bleaching exposure and measurement; some of these transitions occur so rapidly as to require for their detection spectrophotometers capable of nanosecond resolution (Cone, 1972).

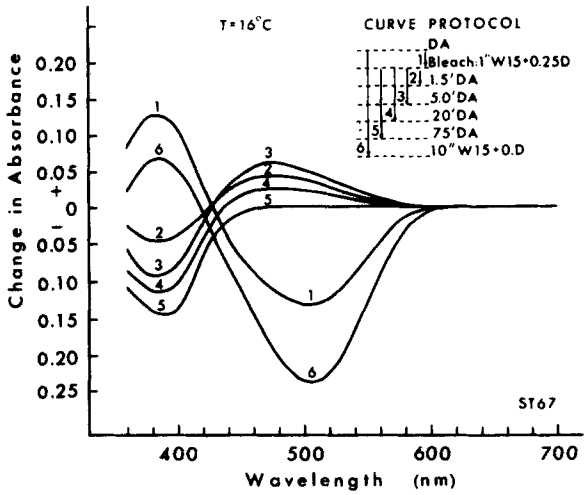

FIGURE 1. Density difference spectra obtained by transmission measurements of a skate retina perfused in aspartate Ringer solution. The legend indicates the times at which spectral measurements were taken and between which the density differences were calculated. Thus, curve 1 shows the bleaching difference spectrum produced by a 1-s exposure to a yellow (Wratten 15) light delivering a retinal illuminance of 0.28 log mW/cm^2; curve 4 shows the spectral changes occurring during the first 20 min after the exposure; and curve 6 shows the density changes occurring between times immediately before the bleaching exposure and immediately after a final, exhaustive bleach.

Curves (2) to (5) of Fig. 1 illustrate the changes in absorbance that took place as the photoproducts continued to undergo thermal changes in the dark; after 75 min of dark adaptation no further change could be detected. During this dark period, the absorbance in the blue region of the spectrum (e.g., 380 nm) decreased continuously, losing approximately the same optical density as that gained initially during the first few seconds after photic exposure. Since both MII and retinal exhibit similar absorption characteristics, this change may represent more than one step in the bleaching sequence.

The results of Fig. 1 reveal also the formation and decay of another photoproduct. Note that spectral curves (2) and (3) show the accumulation of a substance that absorbs maximally at about 470 nm, but that curve (4) indicates a reduction in its concentration, and curve (5) its disappearance. This thermal

intermediate is almost certainly MIII (λ_{max} = 465 nm), which has been shown to participate in the rhodopsin decay sequence both in vitro (Ostroy et al., 1966; but cf. Matthews et al., 1963) and *in situ* (Weale, 1957; Frank, 1969; Ripps and Weale, 1969; Baumann, 1972; Donner and Hemilä, 1975).

The final curve (6) of Fig. 1 is the difference spectrum for transmissivity measurements taken before the flash and those obtained 75 min later, when the retina was exposed to an illumination that bleached completely the remaining rhodopsin. Comparing the absorbance values of this curve with those of curve (1) indicates that the initial exposure bleached 59% of the available rhodopsin.

KINETICS The difference spectra of Fig. 1 show that, in the dark, absorbance changes are most prominent in the regions of 380 nm and 470 nm, wavelengths which are near the absorption peaks of the late photoproducts. Data taken from the same experiment as in Fig. 1 are plotted in Fig. 2*b* to show the changes in absorbance at these wavelengths as functions of time after the bleaching exposure. The values for 470 nm can be described by two exponential functions representing the formation and decay of MIII, the only late photoproduct to absorb significantly in this spectral region. The measurements at 380 nm, however, follow a more complex course. The absorbance values fall rapidly at first, but after 5 min the rate of decline decreases markedly and soon becomes even slower than at 470 nm; a possible cause of this complexity was mentioned earlier. A number of test runs, performed at the same temperature, showed that the results in Figs. 1 and 2 are highly reproducible, and that the kinetics are independent of the fraction of the rhodopsin bleached when 22–87% of the available rhodopsin is isomerized. For smaller bleaches, the kinetics may be different (Donner and Hemilä, 1975).

Analysis of the experimental data shown in Fig. 2 yielded rate constants and absorbance coefficients $(\delta_i)_\lambda$ which, when substituted in the equations derived for the dual pathway decay scheme, generated the curves drawn through the symbols. Although Fig. 2 illustrates the results obtained at T = 12.5°C, 16°C, and 20.5°C, the equations proved equally applicable to measurements taken over a temperature range from 7° to 27°C. The fact that the theoretical equations describe so well the experimental data is evidence that the absorbance changes at 470 nm represent the formation and decay of MIII, whereas $(\Delta D)_{380}$ is due primarily to changes in MII and retinal.

When the appropriate rate constants and absorbance coefficients are substituted in the theoretical equations, the solutions give the temporal changes that each photoproduct undergoes after the isomerizing flash. Fig. 3 shows graphically the solutions for data obtained at 16°C, for which the rate constants were $k_1 = 0.42 \times 10^{-2}\ s^{-1}$, $k_2 = 0.11 \times 10^{-2}\ s^{-1}$, $k_3 = 0.32 \times 10^{-3}\ s^{-1}$, and $k_4 = 0.25 \times 10^{-2}\ s^{-1}$. Since retinol ($\lambda_{max}$ = 325 nm) absorbs outside the spectral range of the apparatus, the curve showing the formation of retinol was calculated on the assumption that the conversion of a measurable photoproduct to a colorless (undetectable) substance reflects the accumulation of retinol.

In addition to the kinetic data, plotting the density coefficient derived by computer analysis for each test wavelength yields the extinction spectrum of the parent pigment and each of the late photoproducts. Fig. 4 shows that the results

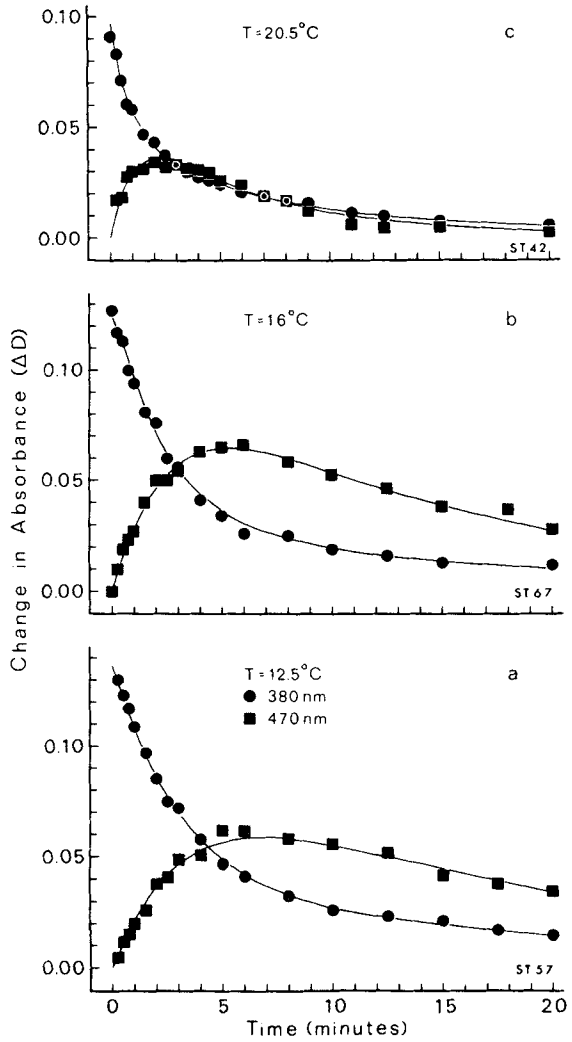

FIGURE 2. Absorbance changes at 380 nm and 470 nm taken from difference spectra recorded during the first 20 min of experimental runs taken at (*a*) 12.5°C, (*b*) 16°C, and (*c*) 20.5°C. Measurements at 380 nm show that absorbance decreased rapidly at first, and then at a slower rate throughout the remainder of the experiment. At 470 nm, absorbance first increased and then decreased, reflecting the exponential accumulation and decay of MIII. The continuous lines are the absorbance changes generated by the computer programs in accordance with the dual pathway model.

calculated for rhodopsin conform almost exactly to the Dartnall nomogram (Dartnall, 1953), and that the spectra depicting the various photoproducts are similar to those obtained from measurements in solution (Matthews et al., 1963; Abrahamson and Ostroy, 1967). It is noteworthy that in the derivation of these spectral curves, no assumptions were made concerning the shapes of the spectra, their peak wavelengths, or the relative concentrations of the various substances.

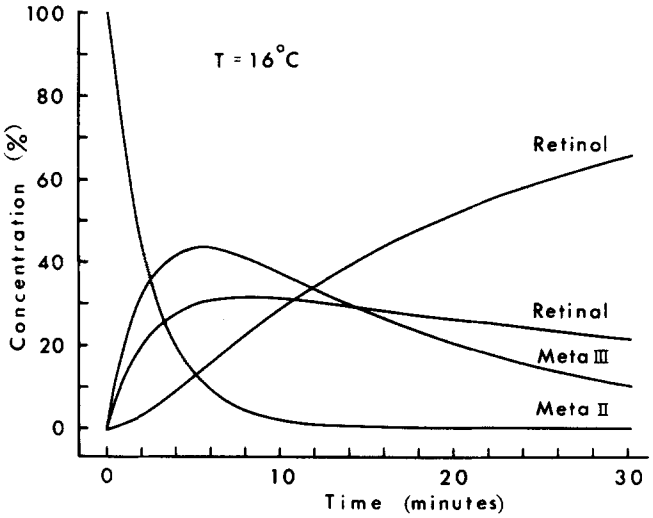

FIGURE 3. Formation and decay of the bleaching intermediates at 16°C based on computer analysis of experimental data fit to the dual pathway model. MII decays exponentially to MIII and retinal, both of which form a product (presumably retinol) undetectable within the spectral range of measurements (360–720 nm).

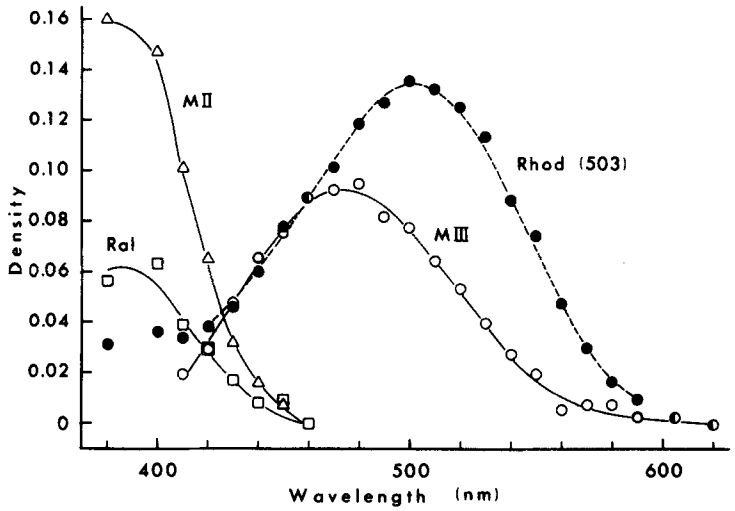

FIGURE 4. Absorbance spectra for the bleaching intermediates derived from the dual pathway model. The curve drawn through the points representing rhodopsin (*Rhod*) was obtained from Dartnall's nomogram for a pigment with λ_{max} = 503 nm; smooth curves are drawn through the remaining points. The curves for MII and MIII correspond closely to the known spectral densities of MII and MIII; the curve for retinal (*Ral*) is less well established.

REACTIONS IN THE DECAY OF LATE PHOTOPRODUCTS It is clear from Figs. 3 and 4 that the model proposed by Cone and Cobbs accounts for that fact that not all of the MII formed after irradiation is converted into MIII. Although the shunt path incorporated in Baumann's model also provides a route by which

MIII is bypassed, the rate constants for the MIII to retinal transition that were required to fit the skate data to the kinetic equations for this scheme were usually small, *negative* values.

Further evidence favoring the "dual pathway" model came unexpectedly from a few experiments in which the thermal reactions did not proceed to completion. Fig. 5, for example, presents the absorbance changes at 470 nm and 380 nm, respectively, for an experimental run at 7°C. The results obtained at 470 nm show the formation and decay of MIII, the rates markedly slowed by the low temperature; i.e. $k_1 = 0.28 \times 10^{-2}\ s^{-1}$, $k_2 = 0.26 \times 10^{-3}\ s^{-1}$. On the other hand, the absorbance data at 380 nm fall along a single exponential curve with a decay

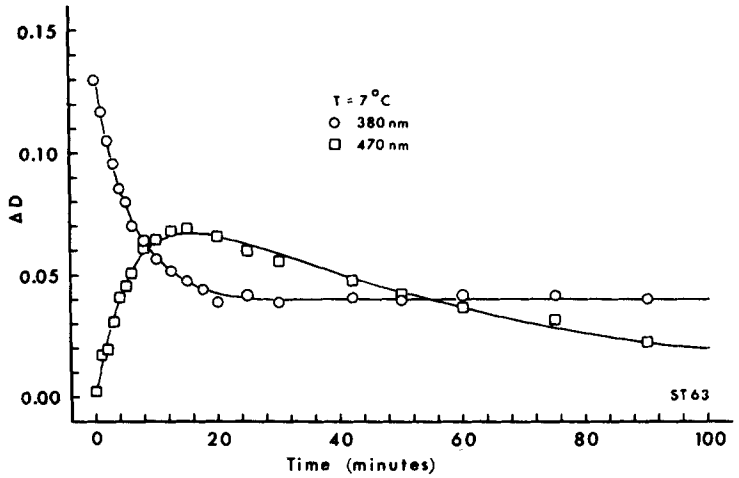

FIGURE 5. Density changes at 380 and 470 nm measured in a preparation in which retinal (λ_{max} = 387 nm) did not decay; i.e., $k_3 = 0$. The curve through the 470-nm squares shows the theoretical formation and decay of MIII. A single exponential decay curve is drawn through the data at 380 nm, representing the decay of MII (see text). Note that after 20 min in darkness there was no change in absorbance at 380 nm despite the fact that the loss of MIII continued throughout the period of measurement.

constant equal to k_1; i.e. the formation of MIII corresponds exactly to the loss of MII. But it can be seen that no detectable change in 380 nm absorbance occurred between 20 min and 100 min, the period during which absorbance measurements at 470 nm declined continuously. Thus, either MIII decayed to an intermediate which did not absorb at 380 nm, or else a product was formed that decayed so rapidly as to go undetected in the measurements. In either event, the photoproduct into which MIII was converted could not have been retinal. Moreover, the failure to detect any decrease in absorbance at 380 nm during the final stages in the decay of MIII supports our contention that changes in MIII do not affect significantly the absorbance measurements at 380 nm.

The plateau that is reached in the 380 nm absorbance data after the decay of MII (Fig. 5), indicates also that some intermediate remained in the retina throughout the final 80 min in darkness. The relevant difference spectra ($\lambda_{max} \approx$

380 nm) suggest that the "stable" photoproduct was probably retinal. It is noteworthy that the sum of the absorbances due to the RAL (0.04) and MIII (0.086) formed during the course of the experiment accounted fully for the absorbance of MII (0.13) that was transformed in the process. This finding, confirmed in experiments in which photoproduct decay ran to completion, suggests that retinal, like MII and MIII, is still oriented optimally with respect to the electric vector of the incident light (Weale, 1973; Kemp, 1973).

EFFECT OF TEMPERATURE The concomitant changes in bleaching kinetics and retinal sensitivity due to variation in temperature are cited frequently as providing support for the view that photoproducts govern the changes in threshold that occur during visual adaptation. Although we will consider later the direct comparison between spectral and electrophysiological data, the effect of temperature on the rate constants of the relevant transitions is illustrated by the Arrhenius plots of Fig. 6. These findings show that temperature variation induces significant changes in the kinetics of each of the thermal reactions with which we are concerned. Although it is possible further to characterize the individual transitions in terms of the parameters of absolute reaction rate theory (Matthews et al., 1963; Ostroy et al., 1966; Ebrey, 1968), a consideration of thermodynamic properties was not dealt with in the present study (but cf. Brin, 1975).

Electrophysiology

Since it was the objective of this investigation to study only receptoral processes, we recorded from the isolated retina and perfused it with Ringer solutions containing sodium aspartate. In addition to precluding rhodopsin regeneration, the absence of the pigmented epithelium eliminates the *c*-wave of the ERG (Noell, 1954), whereas the sodium salt of aspartic acid is an effective agent in suppressing electrical responses that arise proximal to the photoreceptors (Furukawa and Hanawa, 1955; Sillman et al., 1969; Dowling and Ripps, 1971*b*). The resultant waveform (the PIII potential) consists of an initial rapid portion that represents the extracellular expression of the receptoral photocurrent (Penn and Hagins, 1969), and a later slow component that originates most probably in the Müller (glial) cells of the retina (Faber, 1969; Witkovsky et al., 1973; 1975). Our measurements are only of the fast PIII (receptor) response.

Fig. 7 shows electrical responses of an isolated skate retina maintained at 27°C during perfusion with a Ringer solution containing 50 mM Na aspartate. The initial recordings are from a preparation that had been perfused for 80 min in darkness. During the first 8 min of this equilibration period, the maximum voltage that could be elicited (V_{max}) increased by only 4% and absolute threshold decreased by about 0.25 log unit; thereafter, both remained at stable levels. At this time, the responses to relatively dim flashes (log $I_t = -6.5, -5.5$) exhibit only the fast PIII voltage; with brighter flashes, this potential is followed by the slow PIII component. Although the latter is distorted by the time constant (5.5 s) of the preamplifier, it is clear that slow PIII is a prolonged response requiring many seconds to return to the base line.

After a voltage vs. intensity run (V-log I) for the dark-adapted preparation had been obtained, the retina was exposed for 1 s to the unattenuated yellow

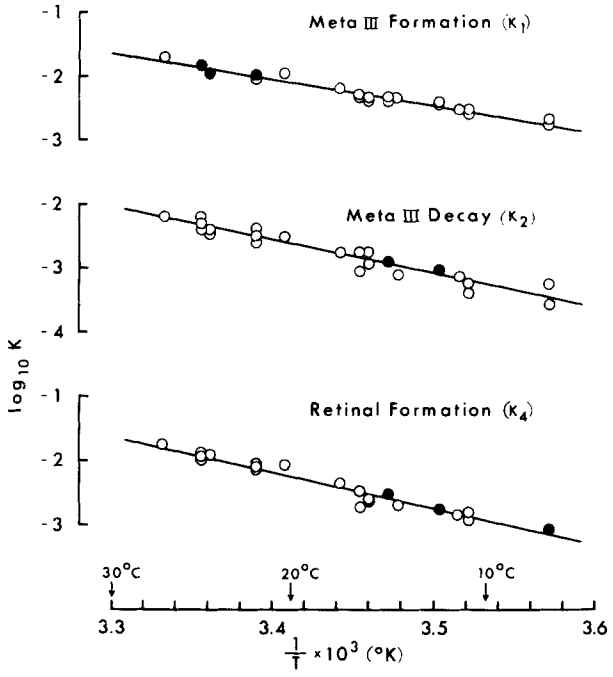

FIGURE 6. Arrhenius plots of the kinetic rate constants for three of the dark reactions incorporated in the dual pathway model. The straight lines were fit by a least-squares method.

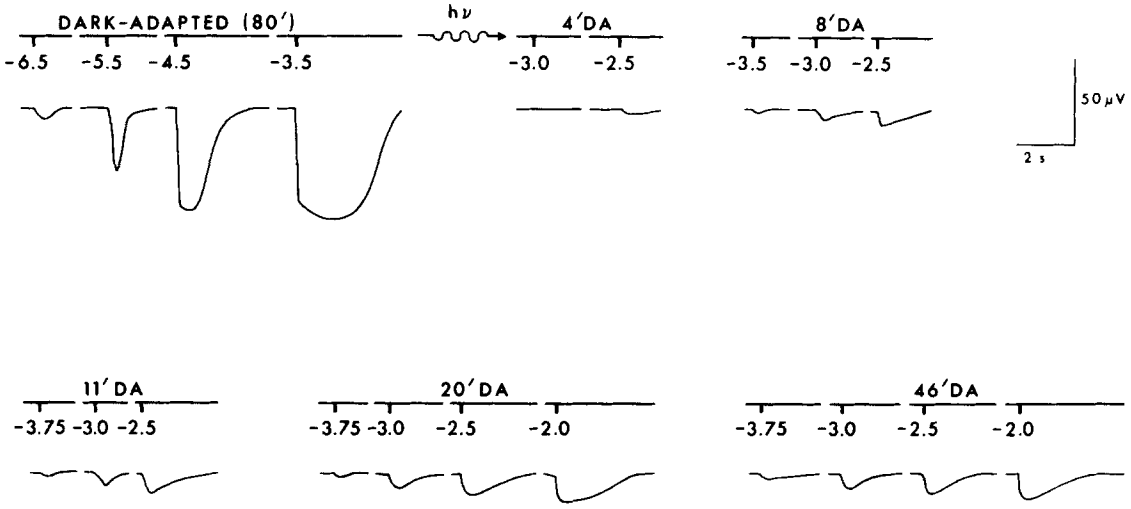

FIGURE 7. The electroretinogram of the aspartate-perfused skate retina during dark adaptation. The ERG test flash, 100 ms in duration, was spectrally shaped by a Wratten 15 (yellow) filter and attenuated by calibrated neutral density filters. The stimulus markings give the flash energy in log mW/cm^2. The first set of recordings was obtained after the retina had been in darkness for 80 min; the remainder were elicited at the times indicated after an exposure which bleached 87% of the available rhodopsin.

bleaching beam (retinal irradiance of 10.0 mW/cm^2), and test flashes were delivered at various times after the bleach. For several minutes after the exposure (the "silent period"), responses could not be elicited with even the brightest flash (Dowling and Ripps, 1970). When the retina was again responsive (the 4′ data of Fig. 7), amplitudes were greatly reduced and threshold markedly elevated as compared with prebleach values. With further time in darkness, thresholds fell and V_{max} increased, but after 87% of the available rhodopsin had been isomerized there was only partial recovery of the two parameters. The lateral displacement of the V-log I curves of Fig. 8 indicates that exposures which

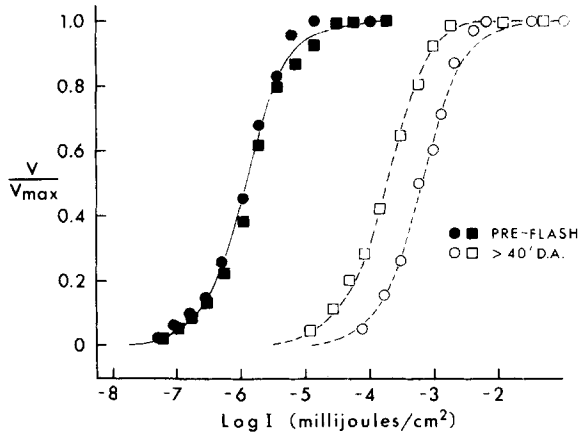

FIGURE 8. Normalized voltage-intensity data for the experiment shown in Fig. 7 (circles), and for another run (squares) in which 45% of the rhodopsin was bleached. The dark-adapted results (filled symbols) are fit by a curve having the form: $V/V_{max} = I^a/(I^a + \delta)$, where I is the intensity of the test flash, $a = 1.1$ is a constant, and δ is the value of I for which the measured voltage (V) is one-half the maximum (V_{max}) that can be elicited under a particular set of experimental conditions. Note that the postbleached data (open symbols) are well fit by the same curve, but displaced to the right on the scale of abscissas, indicating the permanent loss of sensitivity induced by the bleached rhodopsin.

bleached 45% and 87% of the available rhodopsin induced permanent losses in sensitivity of about 2.2 and 2.75 log units, respectively.

Fig. 9 (upper graph) shows the temporal course of threshold recovery during dark adaptation for preparations maintained at the same temperature (27°C) but exposed to pre-adapting flashes of different intensity. Although the duration of the silent period varied in accordance with the efficacy of the bleaching exposure, in each case thresholds fell rapidly at first, declined at a slower rate after about 5 min of dark adaptation, and soon thereafter attained a stable level that was maintained for the remaining time in darkness. Since rhodopsin did not regenerate in these retinas, there was no "photochemical" phase of adaptation. Thus, when thresholds stabilized they were elevated by progressively greater amounts, the larger the fraction of rhodopsin bleached.

RELATION TO PHOTOCHEMICAL EVENTS Spectral transmissivity data obtained in the course of the experiments described above were fit by the computer program to the dual-pathway model to provide the lower curves of Fig. 9 showing the formation and decay of the late photoproducts. Since the experi-

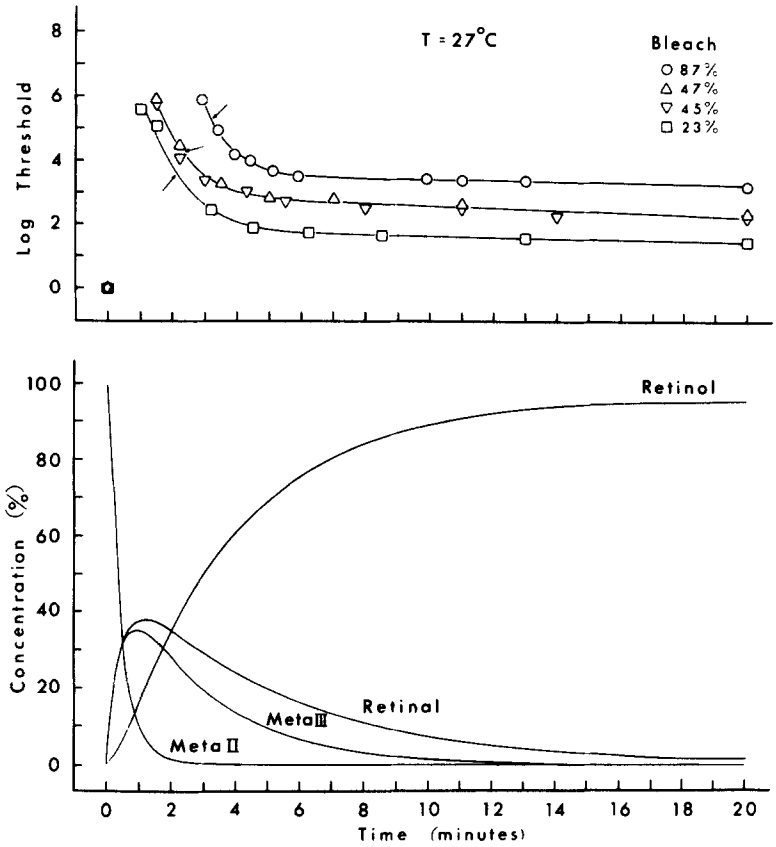

FIGURE 9. Receptoral thresholds (upper half) and photoproduct concentrations (lower half) during dark adaptation. For each experimental run, the initial light exposure bleached a different fraction of rhodopsin. Threshold measurements in the upper graphs reveal a silent period, a period of rapid threshold recovery, and a period of slow threshold recovery. Final thresholds vary with the percent rhodopsin bleached. Arrows indicate approximate times when threshold was elevated by 2 log units above its final level (see text). Photoproduct concentration derived by analysis according to the dual pathway decay sequence is shown in the lower set of curves. Since these experiments differed only in the percent rhodopsin bleached, the photoproduct curves describe the intermediate kinetics for all four preparations.

ments differed only as to the fractional bleaches effected by the pre-adapting exposures, the photoproduct kinetics apply equally to the three experimental conditions of Fig. 9; i.e. the curves give the concentration of each intermediate relative to the fraction of rhodopsin bleached.

Although a correlation between the temporal variation in threshold and the concentration of any of the photoproducts is not immediately apparent, it will be recalled that significant amounts of rhodopsin have been bleached in these experiments, and that this factor alone induces a disproportionately large rise in receptoral threshold (Dowling and Ripps, 1972). Since we wished to consider the changes in threshold that are independent of bleached rhodopsin, it was necessary to subtract out this factor by determining for each bleaching condition the specific times in darkness at which thresholds were elevated by given amounts above the dark-adapted plateau. We could then calculate the concentrations of the bleaching intermediates present within the retina at those particular times. For example, the arrows of Fig. 9 point to the times at which thresholds were elevated by 2.0 log units in each experimental run. If one of the photoproducts is responsible for this threshold rise, its concentration should be the same for the three experimental conditions. The results of Table I indicate that, aside from

TABLE I
CONCENTRATIONS OF PHOTOPRODUCTS

Rhod bleached	Time in dark	MII	MIII	Retinal	Retinol
%	*min*	%	%	%	%
Thresholds 2.0 log units above final threshold					
87	3.2	0.1	16.3	24.8	45.9
46	2.3	0.3	11.9	15.6	18.3
23	2.1	0.3	6.3	8.0	8.4
Thresholds 1.0 log unit above final threshold					
87	3.9	<0.05	12.6	21.7	52.8
46	3.25	<0.05	8.5	13.0	24.5
23	3.1	<0.05	4.5	6.7	11.8

MII, no other photoproduct (or combination of products) provides the consistency needed to establish a quantitative relationship between photoproduct concentration and rod sensitivity. Moreover, Fig. 9 shows that the decay of MIII and retinal continue long after thresholds have stabilized. There is, however, some evidence to suggest a possible link between the rise in threshold and the concentration of MII. In each retina, a 100-fold loss in sensitivity is associated with a MII concentration equal to 0.1–0.3% of the rhodopsin content of the rods. But even this correlation seems fortuitous. When the same computation is carried out for threshold data 1.0 log unit above the dark-adapted plateaus, Table I indicates that MII has fallen to trace amounts (i.e. less than 0.05% of the total rhodopsin).

If MII within the rod outer segments is responsible for the threshold changes during dark adaptation, then our data suggest that skate rods are at least six times more sensitive to this intermediate than are the rods of the frog (Donner and Reuter, 1967). To test whether this relation is maintained when the bleaching kinetics of rhodopsin are altered, similar experiments were performed at various temperatures and in the presence of hydroxylamine. Neither of these maneuvers was without adverse effect on the response characteristics of the transretinal potential. As shown in Fig. 10, a reduction in the temperature of the

perfusate or the addition of hydroxylamine reduced the amplitude of the fast PIII voltage, and prolonged both the rise and decay times of the slow PIII potential. However, these effects were most pronounced with suprathreshold test flashes of high intensity; dark-adapted thresholds were unchanged by hydroxylamine or by a lowering of temperature from 25°C to 15°C.

TEMPERATURE We noted earlier (Fig. 2) that the time course of photoproduct decay in the skate retina is temperature dependent, and the upper half of Fig. 11 reveals that a variation in temperature influences also the temporal course of dark adaptation. In each experimental run, the retina was maintained

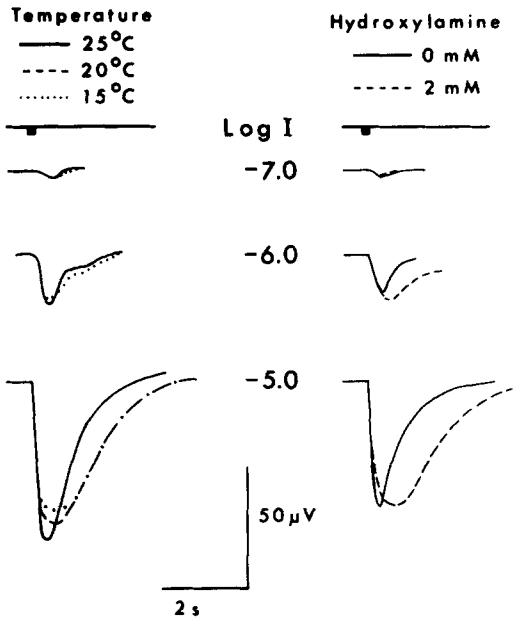

FIGURE 10. The effect of temperature variation and hydroxylamine on electroretinographic responses to different stimulus intensities. The hydroxylamine data were obtained at 20°C.

at a different temperature but exposed to a bleaching flash of the same intensity. Each set of data again displays the rapid and slow phases of recovery that are characteristic of rod adaptation (Fig. 9), and although the "silent" periods were progressively longer as the temperature was lowered, the final thresholds were similar for the three preparations.

The lower half of Fig. 11 shows the MII decay curves for these three experiments. If one applies the same analysis as before, it can be shown that when the threshold for each preparation was 3.0 log units above the plateau that it reached in dark adaptation, the fractions of MII present were 0.005, 0.006, and 0.045 for retinas perfused at 27°C, 22°C, and 12°C, respectively. Although these values exhibit significant variability, it may be argued that due to the small fractions of MII that are involved, and the rapid changes which thresholds are undergoing

at these times, a comparison based on these calculations is equivocal at best. For this reason, we adopted an alternative procedure by which to alter the kinetics of the dark reactions.

HYDROXYLAMINE When rhodopsin is bleached in the presence of hydroxylamine, it leads to the formation of the stable compound retinal oxime, a

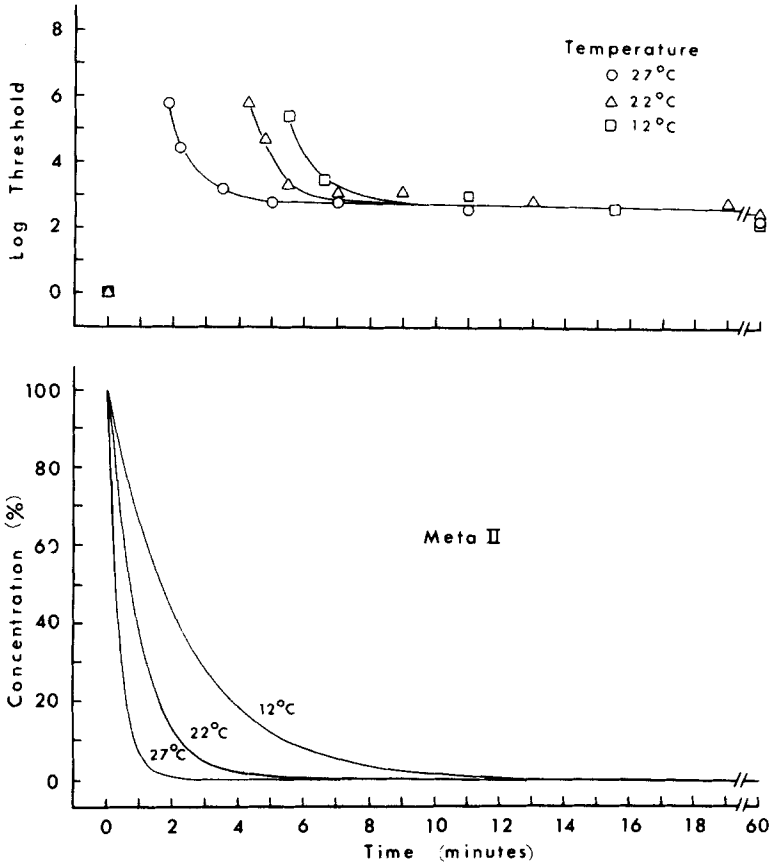

FIGURE 11. The effect of temperature variation on the decay of MII (lower curves) and threshold changes (upper curves) during dark adaptation. In each experimental run, 50% ± 2% of the available rhodopsin was isomerized by the bleaching exposure.

product whose absorption spectrum ($\lambda_{max} \approx 367$ nm) does not interfere with measurements at wavelengths $\geq\lambda_{max}$ of the parent pigment (cf. Wald and Brown, 1953). In addition, it has been shown that the addition of hydroxylamine shortens significantly the lifetimes of the thermal intermediates that are formed during the bleaching sequence (Bridges, 1962; Dartnall, 1968). However, before we could study the effects of this substance, it was necessary to carefully titrate the dose to be administered in the perfusate. Hydroxylamine concentrations in excess of 5 mM proved toxic to the skate retina and the electrical responses

rapidly disappeared; at very low concentrations, the electrical activity was retained, but photoproduct decay was not altered appreciably. At a concentration of 2 mM, however, the photochemical reactions were accelerated, and although the electroretinogram was altered (see Fig. 10), hydroxylamine did not interfere with threshold measurements.

Fig. 12 plots the density changes at 470 nm and 380 nm for two hydroxylamine-perfused retinas maintained at 20°C; both runs were taken after exposure to the same bleaching light. The dashed lines show comparable data from

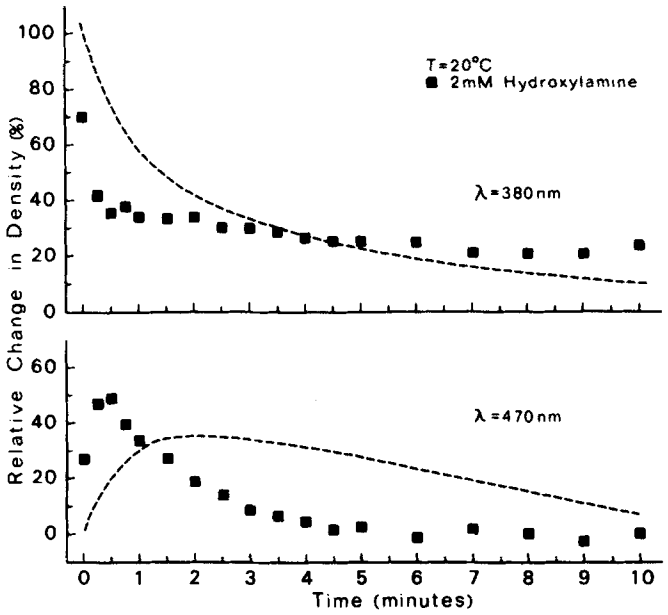

FIGURE 12. Averaged density changes at 380 and 470 nm for skate retinas perfused with Ringer solutions containing 2 mM hydroxylamine. The dashed lines show analogous data from preparations perfused at the same temperature with a control solution lacking hydroxylamine. Absorbance at 380 nm decreased at first much more rapidly in the hydroxylamine-perfused preparations; however, the later measurements at this wavelength reflect the presence of retinyl oxime. The formation and decay of MIII (470 nm data) were also markedly accelerated.

preparations perfused with a hydroxylamine-free aspartate-Ringer solution of the same temperature. Although 2 mM hydroxylamine obviously influences the kinetics of the various transitions, it is difficult to interpret with confidence the density changes at 380 nm, since the build-up of retinyl oxime as well as any changes due to the formation of retinal is reflected in these data. Nevertheless, there can be no confusion as regards the effects of hydroxylamine on MII and MIII; both the decay of MII and the formation and decay of MIII are accelerated markedly by hydroxylamine.

The measurements of receptoral thresholds during dark adaptation gave a very different picture. Fig. 13 shows that after identical photic exposures the

recovery of threshold followed the same time course in the perfusate containing hydroxylamine as in a control solution.

DISCUSSION

It has been possible in this study to identify spectrophotometrically the late photoproducts that form after photic exposure of the isolated, perfused skate retina, and to determine by computer-assisted analytical methods the kinetic parameters associated with these thermal events. In order to determine whether changes in the concentration of the bleaching intermediates are responsible for the changes in rod sensitivity that occur during dark adaptation, we compared the kinetics of the late thermal reactions with the time course of threshold recovery after photic exposure. Although several bleaching protocols and a variety of temperatures were employed (Figs. 9 and 11), the question was not resolved conclusively by these means. Contrary to the results obtained in frog

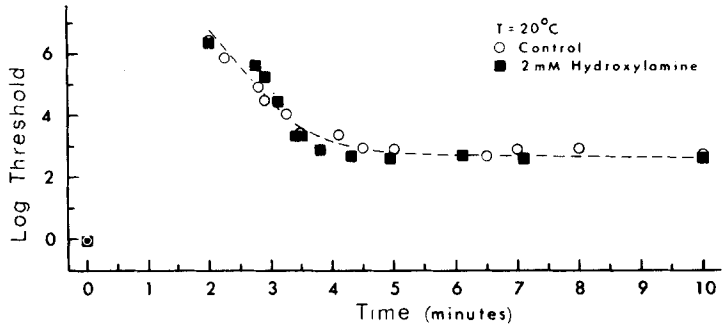

FIGURE 13. Averaged thresholds during dark adaptation from preparations (Fig. 12) perfused with and without 2 mM hydroxylamine. The dashed line, which describes well the two sets of data, shows that threshold recovery is similar for both conditions.

(Frank, 1971), the temporal course of receptor adaptation was clearly affected by changes in temperature. In addition to slowing the decay of the late photoproducts, lowering the temperature of the perfusate delayed the onset of dark adaptation (cf. Fig. 11). However, quantitative analysis of the results revealed a number of inconsistencies between the kinetics of the two processes. Since there is often considerable variability associated with threshold determinations, particularly when sensitivity is changing rapidly, the failure to obtain a perfect correlation cannot be considered an unequivocal finding. Nevertheless, the addition of 2 mM hydroxylamine to the perfusate effectively dissociated the two phenomena and produced a relatively clear-cut result. As compared to measurements obtained in normal Ringer solutions, hydroxylamine greatly accelerated the kinetics of photochemical decay but it had no significant effect on the rate at which rod sensitivity returned during dark adaptation. Thus, it appears that insofar as the sensitivity of skate rods is concerned, the late bleaching intermediates do not provide the rate-limiting factor in the processes that control threshold changes during dark adaptation.

As regards the routes of photoproduct decay, the dual-pathway model of Cone and Cobbs (1969) seems to describe best the results of the present work. Their scheme, formulated originally to describe the bleaching of rhodopsin in the rat retina, incorporates two pathways by which MII is degraded to retinol: one via MIII, the other through retinal. Computer simulation of the model yielded rate constants and spectral absorbance coefficients for the late intermediates in skate which fit experimental data obtained at temperatures ranging from 7°C to 27°C (cf. Fig. 2).

Since it provides a pathway by which MII can bypass MIII, the Cone and Cobbs model readily accommodates the fact that not all of the MII formed after a light flash is converted to MIII (Fig. 4). Moreover, the existence of a MIII bypass helps to resolve a difficulty encountered in the study of human rhodopsin. On the basis of data from fundus reflectometry, Ripps and Weale (1969) derived the absorbance spectrum of MIII, its relative density *in situ*, and the time constants of its formation and decay. Although their spectral curve accurately described MIII, the maximum absorbance attained by this intermediate was only 0.3 that of the rhodopsin which had been isomerized. Since the extinction coefficients of these two species are approximately equal (Matthews et al., 1963), they suggested the possibility that during the formation of MIII the chromophore rotates out of the plane of the disk membrane. It will be recalled that Schmidt (1938) had demonstrated that rhodopsin *in situ* exhibits linear dichroism owing to the orientation of its chromophore with respect to the long axis of the rod outer segment; i.e., the molecules are in the optimal position to absorb the electric vector of light as it normally enters the intact eye. Thus, Ripps and Weale were suggesting that a rotational movement of the chromophore from its original plane of orientation might have led to an apparent decrease in the concentration of MIII. Recently, however, two independent investigations have shown that the orientation of the chromophore is not substantially altered at the MIII stage (Kemp, 1973; Weale, 1973). It would appear, therefore, that the absorbance of MIII calculated by Ripps and Weale (1969) reflected the actual in vivo concentration of this intermediate; i.e. not all of the rhodopsin that had been photically isomerized was converted to MIII in the course of bleaching.

We also tested whether an alternative scheme, proposed by Baumann (1972) and referred to earlier as the shunt model, could account for the results obtained in the skate. However, the kinetic equations which represent Baumann's model did not provide as satisfactory a fit to the spectrophotometric data for the various transitions, nor could this model account for the results obtained in those few experiments in which retinal was not reduced to vitamin A (Fig. 5). We were unable to determine why the reactions were arrested before the formation of retinol, but it is possible that in these instances the continuous perfusion depleted the retina of an essential coenzyme, e.g., NADH (Wald and Hubbard, 1949) or NADPH (Futterman, 1963). Regardless of the cause, the notion that all of the MII formed during photolysis is converted subsequently to retinal (whether directly or via MIII) is incompatible with the results of Fig. 5. According to Baumann's model, the continuous loss of MIII (represented by the 470 nm data) for times greater than 20 min should result in the accumulation of

retinal, and thereby produce a continuous increase in absorbance at 380 nm. The fact that the absorbance at 380 nm remained constant during the decay of MIII indicates that MIII is being transformed into a colorless photoproduct, and suggests a direct transition from MIII to retinol; this route is an integral component of the dual pathway model.

APPENDIX

Transformation of Variables

The mathematical expressions describing absorbance changes in accordance with the dual pathway model contain parameters which are not mutually independent; e.g., $(\delta_{MIII})_{470}$ and k_1 in Eq. (10), and $(\delta_{RAL})_{380}$ and k_4 in Eq. (11). The difficulty can be resolved by a change in variables so that for any test wavelength λ:

$$(\delta^*_{MIII})_\lambda = (\delta_{MIII})_\lambda \times \frac{k_1}{k_1 + k_4},$$

$$(\delta^*_{RAL})_\lambda = (\delta_{RAL})_\lambda \times \frac{k_4}{k_1 + k_4},$$

and

$$k^* = k_1 + k_4.$$

After one has applied regression analysis to solve the absorbance functions for these composite parameters, all that remains is to partition k^* into its components k_1 and k_4. This is simplified by the fact that the extinction coefficients of MII, MIII, and retinal at their respective absorption peaks are approximately equal (Matthews et al., 1966). Hence,

$$(\delta_{MII})_{380} \simeq (\delta_{MIII})_{470} = (\delta^*_{MIII})_{470} \times \frac{k_1 + k_4}{k_1}.$$

k_1 can be calculated from the values of the parameters obtained directly from the iterative procedure:

$$k_1 = k^* \left\{ \frac{(\delta^*_{MIII})_{470}}{(\delta_{MII})_{380}} \right\}.$$

Knowing the value of k_1 enables one to determine the absorbance coefficient of MIII at any wavelength λ:

$$(\delta_{MIII})_\lambda = \frac{k^*}{k_1} \times (\delta^*_{MIII})_\lambda.$$

The analogous equations for k_4 and $(\delta_{RAL})_\lambda$ are:

$$k_4 = k^* \left\{ \frac{(\delta^*_{RAL})_{380}}{(\delta_{MII})_{380}} \right\}$$

$$(\delta_{RAL})_\lambda = \frac{k^*}{k_4} \times (\delta^*_{RAL})_\lambda.$$

We are grateful to Drs. J. E. Dowling and W. G. Owen for discussion and helpful suggestions with regard to the manuscript, to Miss. J. Zakevicius for technical assistance and the preparation of the illustrations, and to Mr. B. Bruno for the design and construction of apparatus.

This study was supported by a Research Grant (EY-00285) from the National Eye Institute, United States Public Health Service.

Received for publication 20 July 1976.

REFERENCES

ABRAHAMSON, E. W., and S. E. OSTROY. 1967. The photochemical and macromolecular aspects of vision. *Prog. Biophys. Mol. Biol.* **17**:179–215.

BAUMANN, CH. 1972. Kinetics of slow thermal reactions during the bleaching of rhodopsin in the perfused frog retina. *J. Physiol. (Lond.).* **222**:643–664.

BRIDGES, C. D. B. 1962. Studies on flash photolysis of visual pigments. IV. Dark reactions following the flash-irradiation of frog rhodopsin in suspensions of isolated photoreceptors. *Vision Res.* **2**:215–232.

BRIN, K. P. 1975. Rhodopsin photoproduct kinetics and "neural" adaptation in the skate retina. Ph.D. Dissertation. New York University School of Medicine, New York.

CONE, R. A. 1972. Rotational diffusion of rhodopsin in the visual receptor membrane. *Nat. New Biol.* **236**:39–43.

CONE, R. A., and W. H. COBBS. 1969. Rhodopsin cycle in the living eye of the rat. *Nature (Lond.).* **221**:820–822.

DARTNALL, H. J. A. 1953. The interpretation of spectral sensitivity curves. *Br. Med. Bull.* **9**:24–30.

DARTNALL, H. J. A. 1968. The photosensitivities of visual pigments in the presence of hydroxylamine. *Vision Res.* **8**:339–358.

DONNER, K. O. 1973. Rod dark-adaptation and visual pigment photoproducts. *In* Biochemistry and Physiology of Visual Pigments. H. Langer, editor. Springer-Verlag, Berlin.

DONNER, K. O., and S. HEMILÄ. 1975. Kinetics of long-lived rhodopsin photoproducts in the frog retina as a function of the amount bleached. *Vision Res.* **15**:985–995.

DONNER, K. O., and T. REUTER. 1967. Dark-adaptation processes in the rhodopsin rods of the frog's retina. *Vision Res.* **7**:17–41.

DONNER, K. O., and T. REUTER. 1968. Visual adaptation of the rhodopsin rods in the frog's retina. *J. Physiol. (Lond.).* **199**:59–87.

DOWLING, J. E. 1963. Neural and photochemical mechanisms of visual adaptation in the rat. *J. Gen. Physiol.* **46**:1287–1301.

DOWLING, J. E., and H. RIPPS. 1970. Visual adaptation in the retina of the skate. *J. Gen. Physiol.* **56**:491–520.

DOWLING, J. E., and H. RIPPS. 1971*a*. S-potentials in the skate retina. *J. Gen. Physiol.* **58**:163–189.

DOWLING, J. E., and H. RIPPS. 1971*b*. Aspartate isolation of receptor potentials in the skate retina. *Biol. Bull. (Woods Hole).* **141**:384–385.

DOWLING, J. E., and H. RIPPS. 1972. Adaptation in skate photoreceptors. *J. Gen. Physiol.* **60**:698–719.

DRAPER, N. R., and H. SMITH. 1966. Applied Regression Analysis. John Wiley & Sons, Inc., New York.

EBREY, T. G. 1968. The thermal decay of the intermediates of rhodopsin *in situ*. *Vision Res.* **8**:965–982.

FABER, D. 1969. Analysis of the slow transretinal potentials in response to light. Ph.D. Dissertation. State University of New York at Buffalo.

FRANK, R. N. 1969. Photoproducts of rhodopsin bleaching in the isolated, perfused frog retina. *Vision Res.* **9**:1415–1433.

FRANK, R. N. 1971. Properties of "neural" adaptation in components of the frog electroretinogram. *Vision Res.* **11**:1113–1123.

FRANK, R. N., and J. E. DOWLING. 1968. Rhodopsin photoproducts: effects of ERG sensitivity in isolated perfused rat retina. *Science (Wash. D. C.)*. **161**:487–489.

FURUKAWA, T., and I. HANAWA. 1955. Effects of some common cations on electroretinogram of the toad. *Jpn. J. Physiol.* **5**:289–300.

FUTTERMAN, S. 1963. Metabolism of the retina. III. The role of reduced triphosphopyridine nucleotide in the visual cycle. *J. Biol. Chem.* **238**:1145–1150.

KEMP, C. M. 1973. Dichroism in rods during bleaching. *In* Biochemistry and Physiology of Visual Pigments. (H. Langer, editor). Springer-Verlag, Berlin.

MATTHEWS, R. G., R. HUBBARD, P. K. BROWN, and G. WALD. 1963. Tautomeric forms of metarhodopsin. *J. Gen. Physiol.* **47**:215–240.

NOELL, W. K. 1954. The origin of the electroretinogram. *Am. J. Ophthal.* **38**:78–90.

OSTROY, S. E., F. ERHARDT, and E. W. ABRAHAMSON. 1966. Protein configuration changes in the photolysis of rhodopsin. II. The sequence of intermediates in thermal decay of cattle metarhodopsin *in vitro*. *Biochim. Biophys. Acta.* **112**:265–277.

PENN, R. D., and W. A. HAGINS, 1969. Signal transmission along retinal rods and the origin of the electroretinographic a-wave. *Nature (Lond.)*. **223**:201–205.

RIPPS, H. and A. G. SNAPPER. 1974. Computer analysis of photochemical changes in the human retina. *Comp. Biol. Med.* **4**:107–122.

RIPPS, H., and R. A. WEALE. 1969. Rhodopsin regeneration in man. *Nature (Lond.)*. **222**:775–777.

SCHMIDT, W. J. 1938. Polarisationsoptische Analyse eines Eiwess-Lipoid-Systems, erläutert am Aussenglied der Sehzellen. *Kolloidzsche.* **85**:137–148.

SICKEL, W. 1965. Respiratory and electrical responses to light stimulation in the retina of the frog. *Science (Wash. D. C.)*. **148**:648–651.

SILLMAN, R. J., H. ITO, and T. TOMITA. 1969. Studies on the mass receptor potential of isolated frog retina. I. General properties of the response. *Vision Res.* **9**:1435–1442.

WALD, G., and P. K. BROWN. 1953. The molar extinction of rhodopsin. *J. Gen. Physiol.* **37**:189–200.

WALD, G., and R. HUBBARD. 1949. The reduction of retinene to vitamin A, *in vitro*. *J. Gen. Physiol.* **32**:367–389.

WEALE, R. A. 1957. Observations on photochemical reactions in living eyes. *Br. J. Ophthalmol.* **41**:461–474.

WEALE, R. A. 1973. Metarhodopsin III. *In* Biochemistry and Physiology of Visual Pigments. H. Langer, editor. Springer-Verlag, Berlin.

WITKOVSKY, P., F. E. DUDEK, and H. RIPPS. 1975. The slow PIII component of the carp electroretinogram. *J. Gen. Physiol.* **65**:119–134.

WITKOVSKY, P., J. NELSON, and H. RIPPS. 1973. Action spectra and adaptation properties of carp photoreceptors. *J. Gen. Physiol.* **61**:401–423.